itive SST anomalies over the tropical South Atlantic and Indian Oceans, as well as to El Niño–Southern Oscillation events (*28*). The heavy rains of 1961–1962 provide a modern analog for the abrupt, high-amplitude $\delta^{18}O_{diatom}$ minima. In November 1961, for example, the precipitation on the footslopes of Mt. Kenya exceeded 275% of normal (*28*) as a result of onshore flow from a large area of anomalously warm SSTs in the western Indian Ocean. Evaporation was also greatly reduced by dense cloud (*29*). A 145-year tree-ring study from Narok Mau, Kenya, confirms a 30 per mil decrease in mean δD, which is highly correlated with $\delta^{18}O$ (*24*) from 1953–1958 to 1959–1963 (*30*).

The importance of moisture balance in causing the $\delta^{18}O_{diatom}$ minima is supported by the pollen evidence for wetter and/or warmer conditions (Fig. 3). Notwithstanding a modest increase in plant cover, unusually heavy precipitation may have led to severe erosion of exposed volcanic soils on Mt. Kenya (*31*), resulting in the magnetic-susceptibility peaks. Our data suggest that anomalously heavy snowfall on the peaks of Mt. Kenya may contribute to the neoglacial ice advances dated >5.7 ka, 3.2 to 2.3 ka, and 1.3 to 1.2 ka (*6*). Lake-level curves from the East African–South Asian monsoon region (*32, 33*) support our climatic interpretation of the $\delta^{18}O_{diatom}$ data (Fig. 3), as does pollen evidence for generally wetter and warmer conditions in Kenya at ~6.8 ka (*34*). Environmental changes on Mt. Kenya are therefore symptomatic of the same climatic-forcing mechanisms that affected low-altitude tropical areas.

We conclude that centennial- to millennial-scale fluctuations in the ^{18}O content of diatom silica from alpine lakes on Mt. Kenya primarily reflect variations in moisture balance and cloud height, driven by SST anomalies. Hence, they provide a valuable new data source to supplement the sparse and rapidly deteriorating (*7*) isotopic archives in tropical glaciers.

References and Notes

1. J. C. Stager, P. A. Mayewski, *Science* **276**, 1834 (1997).
2. L. G. Thompson *et al.*, *Science* **282**, 1858 (1998).
3. S. Hastenrath, *The Glaciers of Equatorial East Africa* (Reidel, Dordrecht, Netherlands, 1981).
4. L. G. Thompson, in *Sea Level, Ice and Climatic Change*, I. Allison, Ed. (IAHS, Canberra, 1979), vol. 131, pp. 55–64.
5. M. Rietti-Shati, A. Shemesh, W. Karlén, *Science* **281**, 980 (1998).
6. W. Karlén *et al.*, *Ambio* **28**, 409 (1999).
7. L. G. Thompson, E. Mosley-Thompson, K. A. Henderson, *J. Quat. Sci.* **15**, 377 (2000).
8. C. K. Gatebe, P. D. Tyson, H. Annegarn, S. Piketh, G. Helas, *J. Geophys. Res.* **104**, 14237 (1999).
9. The ^{14}C dates were measured on total organic carbon and calibrated to give calendar ages using CALIB 3.0. A table of ^{14}C dates is available at *Science* Online (www.sciencemag.org/cgi/content/full/292/5525/2307/DC1). The chronology has been interpolated using a third-order polynomial regression model. For SHT, the regression equation is $y = 0.00006x^3 - 0.039x^2 + 24.747x + 524.2$, $r^2 = 0.994$, and for ST, $y = 0.00012x^3 + 0.071x^2 + 11.227x + 1041.2$, $r^2 = 0.996$, where x is core depth (cm) and y is calendar age before the present. The mud-water interface was not recovered, and ages above the youngest ^{14}C date should be treated with caution.
10. Standard methods were used for the analysis of diatoms, pollen, and magnetic susceptibility (*13*). See also D. L. Swain, thesis, University of Wales, Swansea (1999).
11. Diatom silica was concentrated (to >98%) by chemical cleaning, sieving, and differential settling. The determination of $\delta^{18}O_{diatom}$ included outgassing and prefluorination, followed by extraction of the inner tetrahedrally bound oxygen by a fluorination method. The results were calibrated against laboratory diatom-standard materials and NBS28 international standard quartz, and are reported against Vienna standard mean ocean water (VSMOW). Samples were analyzed up to three times, giving a mean reproducibility of ±0.3 per mil at 1σ. The laboratory diatom standard had a mean variance of ±0.3 per mil, and standard NBS28 had a variance of ±0.1 per mil (both at 1σ), over the period of analysis.
12. W. Vyverman, K. Sabbe, *J. Paleolimnol.* **13**, 65 (1995).
13. F. A. Street-Perrott *et al.*, *Science* **278**, 1422 (1997).
14. K. Rozanski, L. Araguas-Araguas, R. Gonfiantini, in *Climate Change in Continental Isotopic Records*, P. K. Swart, K. C. Lohmann, J. McKenzie, J. Savin, Eds. (American Geophysical Union, Washington, DC, 1993) pp. 1–36.
15. K. Rozanski, L. Araguas-Araguas, R. Gonfiantini, in *The Limnology, Climatology and Paleoclimatology of the East African Lakes*, T. C. Johnson, E. O. Odada, Eds. (Gordon and Breach, Amsterdam, 1996), pp. 79–93.
16. P. M. Grootes, M. Stuiver, L. G. Thompson, E. Mosley-Thompson, *J. Geophys. Res.* **94**, 1187 (1989).
17. M. E. Brandriss, J. R. O'Neil, M. B. Edlund, E. F. Stoermer, *Geochim. Cosmochim. Acta* **62**, 1119 (1997).
18. M. Schmidt *et al.*, *Geochim. Cosmochim. Acta* **65**, 201 (2001).
19. G. Hoffmann, M. Heimann, *Quat. Int.* **37**, 115 (1997).
20. J. Jouzel, G. Hoffmann, R. D. Koster, V. Masson, *Quat. Sci. Rev.* **19**, 363 (2000).
21. J. Duplessy, J. Moyes, C. Pujol, *Nature* **286**, 479 (1980).
22. International Atomic Energy Agency and World Meteorological Organisation, *Global Network for Isotopes in Precipitation (GNIP) and Isotope Hydrology Information System (ISOHIS)* (http://isohis.iaea.org).
23. R. Njitchoua *et al.*, *J. Hydrol.* **223**, 17 (1999).
24. W. G. Darling, thesis, Open University (1996).
25. L. G. Thompson, S. Hastenrath, B. M. Arnao, *Science* **203**, 1240 (1979).
26. J.-C. Fontes, F. Gasse, J. Andrews, in *Isotopic Techniques in the Study of Past and Current Environmental Changes in the Hydrosphere and Atmosphere* (International Atomic Energy Agency, Vienna, 1993), pp. 231–248.
27. C. Sonzogni, E. Bard, F. Rostek, *Quat. Sci. Rev.* **17**, 1185 (1998).
28. S. E. Nicholson, in *The Limnology, Climatology and Paleoclimatology of the East African Lakes*, T. C. Johnson, E. O. Odada, Eds. (Gordon and Breach, Amsterdam, 1996), pp. 25–56.
29. H. Flohn, *Palaeoecol. Afr.* **18**, 3 (1987).
30. R. V. Krishnamurthy, S. Epstein, *Nature* **317**, 160 (1985).
31. W. M. Ngecu, E. M. Mathu, *Environ. Geol.* **38**, 277 (1999).
32. F. A. Street-Perrott, R. A. Perrott, *Nature* **343**, 607 (1990).
33. F. Gasse, E. Van Campo, *Earth Planet. Sci. Lett.* **126**, 435 (1994).
34. O. Peyron, D. Jolly, R. Bonnefille, A. Vincens, J. Guiot, *Quat. Res.* **54**, 90 (2000).

35. Supported by NERC grant GR3/A9523, radiocarbon allocation 728/1297, and isotope project IP/565/0998. Permission for fieldwork in Kenya was granted by the Office of the President, Nairobi, and supported by the National Museum of Kenya. We thank S. Hastenrath, F. Gasse, and an anonymous reviewer for their constructive comments.

6 February 2001; accepted 21 May 2001

Paleobotanical Evidence for Near Present-Day Levels of Atmospheric CO_2 During Part of the Tertiary

Dana L. Royer,[1]*† Scott L. Wing,[2] David J. Beerling,[3] David W. Jolley,[4] Paul L. Koch,[5] Leo J. Hickey,[1] Robert A. Berner[1]

Understanding the link between the greenhouse gas carbon dioxide (CO_2) and Earth's temperature underpins much of paleoclimatology and our predictions of future global warming. Here, we use the inverse relationship between leaf stomatal indices and the partial pressure of CO_2 in modern *Ginkgo biloba* and *Metasequoia glyptostroboides* to develop a CO_2 reconstruction based on fossil *Ginkgo* and *Metasequoia* cuticles for the middle Paleocene to early Eocene and middle Miocene. Our reconstruction indicates that CO_2 remained between 300 and 450 parts per million by volume for these intervals with the exception of a single high estimate near the Paleocene/Eocene boundary. These results suggest that factors in addition to CO_2 are required to explain these past intervals of global warmth.

Atmospheric CO_2 concentration and temperature have been tightly correlated for the past four Pleistocene glacial-interglacial cycles (*1*). Various paleo-CO_2 proxy data (*2, 3*) and long-term geochemical carbon cycle models (*4–6*) also suggest that CO_2-temperature coupling has, in general, been maintained for the entire Phanerozoic (*7*). Recent CO_2 proxy data, however, indicate low CO_2 values during the mid-Miocene

thermal maximum (*8, 9*), and results for the middle Paleocene to early Eocene, another interval of known global warmth relative to today, are not consistent, ranging from ~300 to 3000 parts per million by volume (ppmv) (*2, 9*). Here, we address this problem by developing and applying an alternative CO_2 proxy based on the inverse correlation between the partial pressure of atmospheric CO_2 and leaf stomatal index (SI), with the aim of reconstructing CO_2 for both intervals to determine its role in regulating global climate.

Most modern vascular C_3 plants show an inverse relationship between the partial pressure of atmospheric CO_2 and SI (*10–12*), a likely response for maximizing water-use efficiency (*10*). SI is calculated as: $SI\ (\%) = [SD/(SD + ED)] \times 100$, where a stoma is defined as the stomatal pore and two flanking guard cells, SD = stomatal density, and ED = non-stomatal epidermal cell density. Since SI normalizes for leaf expansion, it is largely independent of plant water stress, and is primarily a function of CO_2 (*10, 12*). This plant-atmosphere response therefore provides a reliable paleobotanical approach for estimating paleo-CO_2 levels from SI measurements on Quaternary (*13*) and pre-Quaternary fossil leaves (*14*). Because stomatal responses to CO_2 are generally species-specific (*12*), one is limited in paleo-reconstructions to species that are present both in the fossil record and living today. Fossils morphologically similar to living *Ginkgo biloba* and *Metasequoia glyptostroboides* extend back to the Early and Late Cretaceous, respectively, and many workers consider the living and fossil forms conspecific (*15, 16*). In this study, we use *G. adiantoides* and *M. occidentalis*, the forms most closely resembling *G. biloba* and *M. glyptostroboides*, and also *G. gardneri*, which has more prominent papillae and less sinuous upper epidermal cells than *G. biloba* (*16*).

Measurements of SI made on fossil *Ginkgo* and *Metasequoia* were calibrated with historical collections of *G. biloba* and *M. glyptostroboides* leaves from sites that developed during the anthropogenically driven CO_2 increase of the past 145 years and with saplings of *G. biloba* and *M. glyptostroboides* grown in CO_2-controlled greenhouses (*17*). These data show a strong linear reduction in SI for both species between 288 and 369 ppmv CO_2 and a nonlinear response at CO_2 concentrations above 370 ppmv (Fig. 1). Because SI responds to partial pressure, not concentration (*11*), the effects of elevation must be considered. All of the leaves measured for the training set grew at elevations <250 m where concentration ≅ partial pressure, so a correction is not needed. Both nonlinear regressions are highly significant (Fig. 1); however, a discontinuity exists for *Ginkgo* between the experimental results above 350 ppmv and the rest of the calibration set. Many species require more than one growing season for SI to adapt to high CO_2 (*12*), and so these experimental results likely represent maxima for a given CO_2 level. Nevertheless, due to this discontinuity as well as the small sample size and decreased sensitivity at high CO_2 for both *Ginkgo* and *Metasequoia*, paleo-CO_2 estimates >400 ppmv should be considered semi-quantitative.

To reconstruct atmospheric CO_2 changes, we measured the SI of fossil *Ginkgo* and *Metasequoia* cuticles from 24 localities in western North America and one from the Isle of Mull (Scotland), and then calibrated these data against the modern training set (Fig. 1) using inverse regression (*18*). Although not tightly constrained, the paleoelevations for all of the sites were probably <1000 m. This elevation difference could increase our estimates of CO_2 concentration by at most 10%, and so our conversion from partial pressure to concentration excludes any correction. Except for a single high CO_2 value near the Paleocene/Eocene boundary, all of our reconstructed CO_2 concentrations lie between 300 and 450 ppmv (Fig. 2 and Table 1). These contrast with two other *Ginkgo*-based CO_2 estimates for the late Paleocene and middle Miocene (*19, 20*) that are very high (4500 and 2100 ppmv, respectively).

We have *Metasequoia*-derived CO_2 estimates only from the warm interval of the middle Miocene, but these are similar to coeval estimates derived from *Ginkgo* cuticles. The convergence of these two independent estimates increases our confidence that both species are reliably recording paleoatmospheric CO_2 levels. In addition, the measured SI values from most sites fall well inside the region of high CO_2 sensitivity in the training sets (Fig. 1 and Table

[1]Department of Geology and Geophysics, Yale University, Post Office Box 208109, New Haven, CT 06520–8109, USA. [2]Department of Paleobiology, Smithsonian Institution, Washington, DC 20560, USA. [3]Department of Animal and Plant Sciences, University of Sheffield, Sheffield S10 2TN, UK. [4]Centre for Palynology, University of Sheffield, Sheffield S3 7HF, UK. [5]Department of Earth Sciences, University of California, Santa Cruz, CA 95064, USA.

*To whom correspondence should be addressed. E-mail: dana.royer@yale.edu

†Address as of 1 August 2001 will be Department of Animal and Plant Sciences, University of Sheffield, Sheffield S10 2TN, UK.

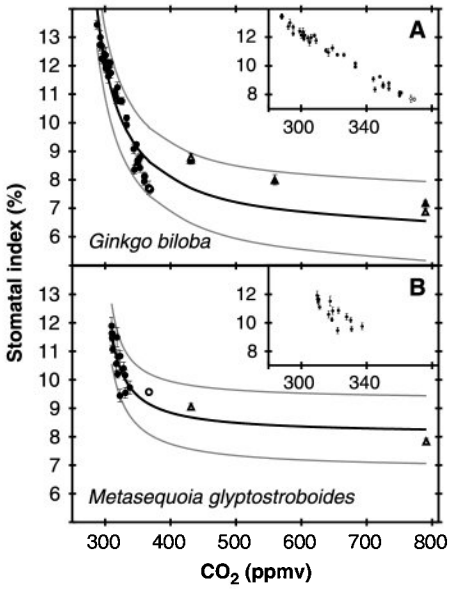

Fig. 1. Training sets for (**A**) *Ginkgo biloba* (n = 40) and (**B**) *Metasequoia glyptostroboides* (n = 18). Thick black lines represent regressions {*Ginkgo*: $r^2 = 0.91$, $F(1,38) = 185$, $P < 0.001$, $SI = [CO_2 - 194.4]/[(0.16784) \times CO_2 - 41.6]$; *Metasequoia*: $r^2 = 0.85$, $F(1,16) = 41$, $P < 0.001$, $SI = [CO_2 - 274.5]/[(0.12373) \times CO_2 - 35.3]$}. Gray lines represent ±95% prediction intervals. Inset graphs show the linear portions of both response curves in greater detail. Stomatal index determined from herbarium sheets (●), fresh samples from living trees (○), and 6- (▲) and 1-year-old (△) saplings growing in CO_2-controlled greenhouses. Error bars represent standard errors.

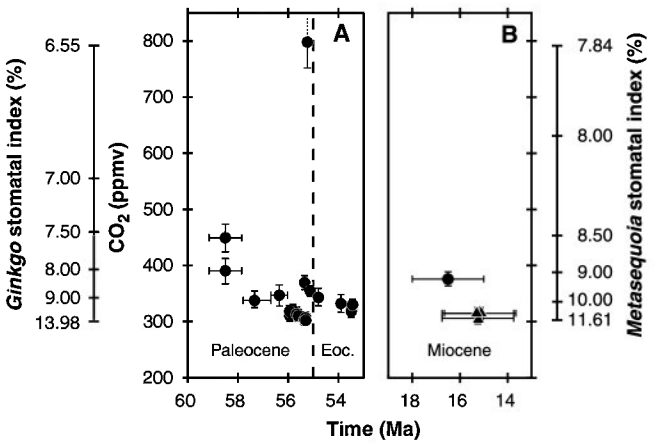

Fig. 2. Reconstruction of paleo-CO_2 for the (**A**) middle Paleocene to early Eocene and (**B**) middle Miocene based on SI measurements from *Ginkgo* (●) and *Metasequoia* (▲) fossil cuticles. Errors represent ±95% confidence intervals.

1), and the 95% confidence intervals (±50 ppmv or less) are over an order of magnitude lower than the errors associated with early Tertiary CO_2 estimates from geochemical models (*4–6*) and other proxies (*2, 9*). Furthermore, middle Paleocene to early Eocene CO_2 reconstructions based on pedogenic carbonate (*2, 21*) and marine boron isotopes (*9*) show large changes in CO_2 (≥2000 ppmv) over geologically brief periods of time [<1 million years] (Fig. 3) that cannot be readily explained. In contrast, the highly constrained error ranges and consistency among near time-equivalent estimates suggest that our SI-derived CO_2 reconstruction is presently the most reliable, particularly for the middle Paleocene to early Eocene.

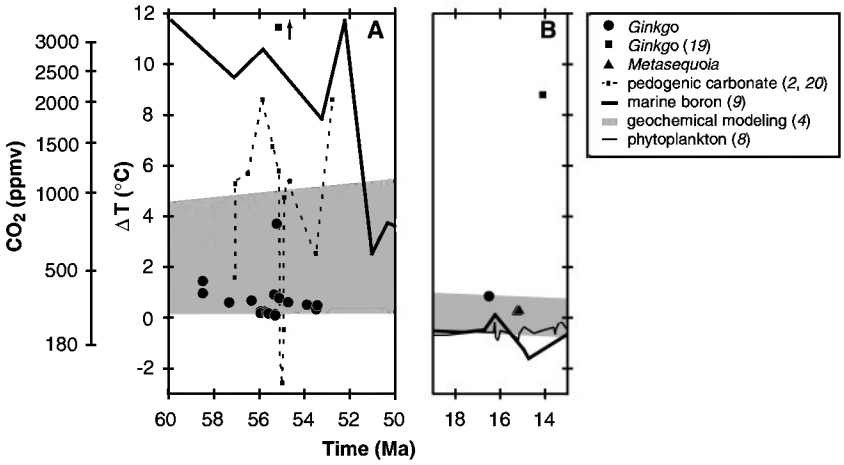

Fig. 3. Estimates of paleo-CO_2 concentration derived from a variety of methods and their corresponding model-determined temperature departures (ΔT) of global mean surface temperature (GMST) from present day for the (**A**) middle Paleocene to early Eocene and (**B**) middle Miocene. Paleo-GMST calculated from paleo-CO_2 estimates using the CO_2-temperature sensitivity study of Kothavala *et al.* (*32*). Present-day reference GMST calculated using the pre-industrial CO_2 value of 280 ppmv (14.7°C). The error range of GMST predicted from the geochemical modeling-based CO_2 predictions of (*4*) corresponds to the model's sensitivity analysis.

Table 1. Summary of fossil data. *n* = number of leaves measured for calculation of SI. A = south-central Alberta (Canada), BHB = Bighorn Basin (Wyoming and Montana, United States), M = Isle of Mull (United Kingdom), I = north-central Idaho (United States). Dashes indicate that no analyses were performed BOM = bulk organic matter, $\delta^{13}C_{om}$ = $\delta^{13}C$ of organic matter. See (*39*) for $\delta^{13}C$ methodology.

Site	Location	Age (Ma)	*n*	SI (%)	CO_2 (ppmv)	$\delta^{13}C_{om}$ (V-PDB)
			Ginkgo			
Burbank	A	58.5	7	7.55	450	–
Joffre Bridge	A	58.5	5	7.96	391	–
SLW 0025	BHB	57.3	7	9.01	340	–
LJH 7132	BHB	56.4	5	8.75	348	–23.91
SLW 991	BHB	55.9	5	10.97	314	–
SLW 992	BHB	55.9	8	10.80	316	–25.66
SLW 993	BHB	55.9	8	11.43	311	–
LJH 72141-1	BHB	55.8	12	10.63	317	–
SLW 9155	BHB	55.7	10	11.21	313	–29.80
SLW 9411	BHB	55.6	8	11.50	311	–23.77
SLW 9434	BHB	55.4	7	12.23	307	–22.53
SLW 9715	BHB	55.3	12	8.23	371	–24.17
SLW 9050	BHB	55.3	5	12.18	308	–26.99
SLW 9936	BHB	55.3	15	11.77	310	–
SLW 8612	BHB	55.3	7	12.41	307	–
Ardtun Head	M	55.2	13	6.54	798	–24.68
AR-2 (BOM)						–24.56
AR-6 (BOM)						–25.82
AR-8 (BOM)						–24.17
AR-10 (BOM)						–24.26
AR-15 (BOM)						–24.54
SLW 9812	BHB	55.1	22	8.53	356	–24.49
SLW 9915	BHB	54.8	8	8.83	345	–
SLW LB	BHB	53.9	5	9.29	334	–
SLW H	BHB	53.5	9	10.22	321	–26.93
LJH 9915	BHB	53.4	15	9.38	332	–26.33
Juliaetta (P6)	I	16.5	14	8.14	377	–
			Metasequoia			
Clarkia (P33a)	I	15.3	6	11.59	307	–
Clarkia (P33b)	I	15.3	10	10.94	316	–
P37a	I	15.2	10	10.95	316	–

A period of rapid climatic warming (~2°C global mean rise within 10^4 years that lasted 10^5 years) near the Paleocene/Eocene boundary has been extensively documented (*22–25*). Although the leading hypothesis for the cause of most of this warming is the rapid release of methane from marine gas hydrates and its subsequent oxidation to CO_2 in the atmosphere and ocean (*25, 26*), all previous attempts to resolve this possible atmospheric CO_2 spike have failed (*23, 27, 28*). Our single high CO_2 estimate is based on *G. gardneri* cuticle from Ardtun Head, Isle of Mull. Anomalously low $\delta^{13}C_{om}$ values (–30‰), an influx of the marine dinocyst *Apectodinium*, and a thermophyllic flora (including *Caryapollenties veripites* and *Alnipollenites verus*) occur in stratigraphically equivalent sediments elsewhere on Mull. Together, these indicate a possible correlation with a section of a Paris Basin borehole that has been calibrated to this event (*29*). At Ardtun Head, however, we failed to capture the negative carbon isotope excursion globally associated with this event, which ranges from 2.5‰ in the deep ocean (*22, 25*) to as much as 6‰ on land (*23*) (Table 1). Although the precise age of the Ardtun Head site remains uncertain, using a global carbon isotope mass balance model calibrated to Paleocene/Eocene conditions (*30*), our reconstructed CO_2 increase (500 ppmv) is consistent with a release of 2522 Gt of methane-derived carbon, a value close to the estimate (2600 Gt C) calculated to account for the marine carbon isotopic excursion using methane as the carbon source (*31*).

Carbon dioxide is an important greenhouse gas, and its effect on global mean surface temperature (GMST) can be quantified with general circulation models (GCMs) [e.g., (*32*)]. Using the model output of Kothavala *et al.* (*32*) we predicted GMST from our CO_2 results. The GCM used by Kothavala *et al.* is calibrated to the present day, which allows us to test the effect of CO_2 on GMST independent of any paleogeographic or vegetational changes. With the exception of the single value near the Paleocene/Eocene boundary, all predictions lie within 1.5°C of the pre-industrial GMST (Fig. 3). These predictions contrast sharply with most paleoclimatic interpreta-

tions for these time intervals. For example, based on a synthesis of global late Paleocene and early Eocene $\delta^{18}O$-derived sea surface temperature data, Huber and Sloan (*24*) estimated that GMST was 3° to 4°C higher than today at this time, and $\delta^{18}O$-derived temperature estimates for the mid-Miocene thermal maximum [17 to 14.5 million years ago (Ma)] indicate that deep and high-latitude surface ocean temperatures were as much as 6°C warmer than today (*33*).

As a cross-check on our results, we compared our GMST predictions with those based on a geochemical carbon cycle model and other CO_2 proxies for these same time periods. With the exception of the one CO_2 estimate by Retallack (*19*), there is very good agreement among the methods for the middle Miocene (Fig. 3), strongly suggesting that factors in addition to CO_2 are required to explain this brief warm period. In contrast, a large disagreement (10°C or greater) exists for the middle Paleocene to early Eocene (Fig. 3). This discrepancy is largely driven by the high CO_2 estimates derived from marine boron isotopes (*9*); however, this proxy is probably less accurate than the other methods (*3, 34*). Nevertheless, even if the boron-based predictions are discounted, a large range still exists among the remaining three methods. This is striking considering that many of the pedogenic carbonate-derived CO_2 estimates are based on the same sediments as our stomatal-based estimates (*21*); however, these estimates show a large temporal variability (−60 to 2040 ppmv) and are associated with relatively large error ranges (±500 ppmv). If our low SI-based temperature predictions are correct, additional factors such as paleogeography, enhanced meridional heat transport, and high latitude vegetation feedbacks are required to explain this warm period, and new constraints for CO_2 levels are established for middle Paleocene/early Eocene and middle Miocene GCMs [e.g., (*35*)]. Understanding the mechanisms of climate change will become increasingly important in the near future as atmospheric CO_2 levels climb to levels perhaps unprecedented for the last 60 My.

References and Notes

1. J. R. Petit *et al.*, *Nature* **399**, 429 (1999).
2. D. D. Ekart, T. E. Cerling, I. P. Montañez, N. J. Tabor, *Am. J. Sci.* **299**, 805 (1999).
3. D. L. Royer, R. A. Berner, D. J. Beerling, *Earth Sci. Rev.*, in press.
4. R. A. Berner, Z. Kothavala, *Am. J. Sci.* **301**, 182 (2001).
5. E. Tajika, *Earth Planet. Sci. Lett.* **160**, 695 (1998).
6. K. Wallmann, *Geochim. Cosmochim. Acta*, in press.
7. T. J. Crowley, R. A. Berner, *Science* **292**, 870 (2001).
8. M. Pagani, M. A. Arthur, K. H. Freeman, *Paleoceanography* **14**, 273 (1999).
9. P. N. Pearson, M. R. Palmer, *Nature* **406**, 695 (2000).
10. F. I. Woodward, *Nature* **327**, 617 (1987).
11. F. I. Woodward, F. A. Bazzaz, *J. Exp. Bot.* **39**, 1771 (1988).
12. D. L. Royer, *Rev. Palaeobot. Palynol.* **114**, 1 (2001).
13. M. Rundgren, D. Beerling, *Holocene* **9**, 509 (1999).
14. J. van der Burgh, H. Visscher, D. L. Dilcher, W. M. Kürschner, *Science* **260**, 1788 (1993).
15. R. W. Chaney, *Trans. Am. Philos. Soc.* **40**, 171 (1951).
16. H. Tralau, *Lethaia* **1**, 63 (1968).
17. Training sets were largely derived from herbarium sheets, where three fields of view (0.1795 mm^2 each) from each of five leaves were measured using epifluorescence (for *Ginkgo*) and transmitted light (for *Metasequoia*) microscopy. Geographic origins of herbarium sheets range from the United States, Japan, and China. During the growing seasons of 1999 (*Ginkgo* and *Metasequoia*) and 2000 (*Ginkgo*), measurements were made on living trees. Reference CO_2 values were taken from the Siple Station ice core (*36*) for the period 1856–1957 and from direct Mauna Loa measurements for the period 1958–2000 (www.cmdl.noaa.gov/ccg/figures/co2mm_mlo.gif). Measurements were also made on *Ginkgo* saplings growing in CO_2-controlled greenhouses after two growing seasons at 350 and 560 ppmv (*37*) and after one growing season for 6- (*Ginkgo*) and 1-year-old (*Ginkgo* and *Metasequoia*) saplings at 430 and 790 ppmv [see (*37*) for experimental methodology]. Fields of view were concentrated near the centers of leaves in the intercostals, which have been shown in other species to yield the least variation in SI (*12*). Although stomata occur in rows in *Metasequoia*, the field of view chosen (0.1795 mm^2) nearly spanned the distance between the midrib and margin, and thus the stomatal bands should not confound our results.
18. Measurements of SI were made on fossil cuticles on each of 5 to 22 leaves per site (Table 1) using epifluorescence (for *Ginkgo*) and transmitted light (for *Metasequoia*) microscopy, with count replication and field sizes as in (*17*). Inverted regression for *Ginkgo*: $CO_2 = [1 - (0.1564) \times SI]/[0.00374 - (0.0005485) \times SI]$, $r^2 = 0.84$, $F(1,38) = 91$, $P < 0.001$; and for *Metasequoia*: $CO_2 = (SI - 6.672)/[(0.003883) \times SI - 0.02897]$, $r^2 = 0.98$, $F(1,16) = 336$, $P < 0.001$. Standard errors in SI for fossil sites are ~0.20%. Fossil *Ginkgo* leaves preserved in environments that today host well-watered, open canopy forests (D. L. Royer, in preparation). Such conditions should minimize both the influence of confounding variables in the SI-CO_2 signal and the environmental differences between the training and fossil data sets. It is possible a species effect on SI exists between *G. gardneri* at Ardtun Head and *G. adiantoides* at the other sites; however, a difference in SI of 6 (Table 1) is highly unlikely based on studies of intrageneric SI variation in modern plants (*12*). All Bighorn Basin sites are dated using Age Model 2 of Wing *et al.* (*38*), while the Ardtun Head site is dated assuming it is stratigraphically near the latest Paleocene carbon isotope excursion (55.2 Ma using Age Model 2). For details of dating methods for the other sites, contact the corresponding author (D.L.R.).
19. G. J. Retallack, *Nature* **411**, 287 (2001).
20. These two CO_2 estimates are based upon small sample sizes ($n = 4$ cuticle fragments each) and an extrapolation of a training set calibrated only up to 560 ppmv.
21. In addition to the published estimates compiled in (*2*), we also made seven new CO_2 estimates based on our record of cuticle $\delta^{13}C$ (Table 1) and the $\delta^{13}C$ of pedogenic carbonate ($\delta^{13}C_{cc}$) from sites stratigraphically within 15 m (~30 ky) of our cuticle-bearing sites (P. L. Koch, in preparation). This affords the rare opportunity to apply multiple CO_2 proxies to sediments in close geographic and stratigraphic proximity. CO_2 calculated using Equation 1 in (*2*) and a planktonic foraminifera-derived atmospheric $\delta^{13}C$ value of −5.6‰, and assuming the concentration of CO_2 contributed by soil = 5000 ppmv and soil temperature = 25°C (*2*). At sites SLW 826, 882, and 8822, we analyzed bulk cuticle, not just *Gingko* cuticle. The site names from which the cuticle and corresponding pedogenic carbonate were collected, $\delta^{13}C_{cc}$ values, and CO_2 estimates (±~500 ppmv) are as follows: LJH 7132, SC 85 and 185, −7.95‰, 1185 ppmv; SLW 992, SC 92, −7.82‰, 2041 ppmv; SLW 9715, SC 22, −7.69‰, 1448 ppmv; SLW 9812, SC 4, −8.36‰, 1217 ppmv; SLW 826 (54.8 Ma, $\delta^{13}C_{om} = -28.65‰$), YPM 200+4m, −11.88‰, 1152 ppmv; SLW 882 (53.5 Ma, $\delta^{13}C_{om} = -27.71‰$) and SLW H and LJH 9915, YPM 320 and D1217+10m, −11.96‰, 577 ppmv; SLW 8822 (52.8 Ma, $\delta^{13}C_{om} = -28.71‰$), Fern Q lower, −10.01‰, 2034 ppmv.
22. J. P. Kennett, L. D. Stott, *Nature* **353**, 225 (1991).
23. P. L. Koch, J. C. Zachos, P. D. Gingerich, *Nature* **358**, 319 (1992).
24. M. Huber, L. C. Sloan, *J. Geophys. Res.* **104**, 16633 (1999).
25. R. D. Norris, U. Röhl, *Nature* **401**, 775 (1999).
26. G. R. Dickens, J. R. O'Neil, D. K. Rea, R. M. Owen, *Paleoceanography* **10**, 965 (1995).
27. L. D. Stott, *Paleoceanography* **7**, 395 (1992).
28. A. Sinha, L. D. Stott, *Global Planet. Change* **9**, 297 (1994).
29. M. Thiry, A. Sinha, L. D. Stott, *Mem. Sci. Terre* **34**, 21 (1998).
30. D. J. Beerling, *Palaeogeogr. Palaeoclimatol. Palaeoecol.* **161**, 395 (2000).
31. G. R. Dickens, in *Natural Gas Hydrates: Occurrence, Distribution, and Detection*, C. K. Paull, W. P. Dillon, Eds. (*Geophys. Monogr. Ser. 124*, American Geophysical Union, Washington, DC, in press).
32. Z. Kothavala, R. J. Oglesby, B. Saltzman, *Geophys. Res. Lett.* **26**, 209 (1999).
33. S. M. Savin, R. G. Douglas, F. G. Stehli, *Geol. Soc. Am. Bull.* **86**, 1499 (1975).
34. D. Lemarchand, J. Gaillardet, É. Lewin, C. J. Allègre, *Nature* **408**, 951 (2000).
35. L. C. Sloan, D. K. Rea, *Palaeogeogr. Palaeoclimatol. Palaeoecol.* **119**, 275 (1995).
36. H. Friedli, H. Lötscher, H. Oeschger, U. Siegenthaler, B. Stauffer, *Nature* **324**, 237 (1986).
37. D. J. Beerling, J. C. McElwain, C. P. Osborne, *J. Exp. Bot.* **49**, 1603 (1998).
38. S. L. Wing, H. Bao, P. L. Koch, in *Warm Climates in Earth History*, B. T. Huber, K. G. MacLeod, S. L. Wing, Eds. (Cambridge Univ. Press, Cambridge, 2000), pp. 197–237.
39. Stable carbon isotope analyses were conducted on *Ginkgo* cuticle fragments at all sites, as well as on bulk organic matter at Ardtun Head. Cuticle fragments were separated from host rock with either tweezers or by placing drops of 52% HF along the cuticle edges. Bulk organic matter was prepared by reacting finely ground host rock with 38% HCl for 6 hours, centrifuging, reacting with fresh HCl for an additional 24 hours, then repeating with 5:1 52% HF:38% HCl. Carbon dioxide was generated for isotopic analysis by combustion in sealed, evacuated VYCOR tubes at 910°C for 1 hour in the presence of CuO and Cu metal. After cryogenic distillation, CO_2 was analyzed on a gas source mass spectrometer. Data are reported relative to V-PDB. Replicate analyses of a laboratory gelatin standard analyzed with these samples had a standard deviation of 0.05‰ ($n = 9$).

40. We thank the Missouri Botanical Garden, National Arboretum, University of California Herbarium, Morris Arboretum, and Brooklyn Botanical Garden for loaning *Ginkgo* and *Metasequoia* herbarium sheets; the British Natural History Museum and University of Alberta for loaning fossil *Ginkgo* cuticle; A. Ash and W. C. Rember for assistance with cuticle preparation and fieldwork; C. P. Osborne for managing the greenhouse experiments; and G. R. Dickens for reviewing a draft. This research was funded by an NSF Graduate Research fellowship (D.L.R.), the Department of Energy grant DE-FGO_2-95ER14522 (D.L.R., R.A.B.), and the Smithsonian Institution (S.L.W.). D.J.B. gratefully acknowledges funding through the Natural Environment Research Council, UK award no. GR3/11900, and a Royal Society University Research Fellowship.

7 March 2001; accepted 21 May 2001